ELSEVIER

Journal of Membrane Science 109 (1996) 43–53

journal of MEMBRANE SCIENCE

Measurement of particle/membrane interactions by a hydrodynamic method

D. Elzo [a,*], P. Schmitz [b], D. Houi [b], S. Joscelyne [a]

[a] *Lund University, Food Engineering, P.O. Box 124, S-22100, Lund, Sweden*

[b] *Institut de Mecanique des fluides, Avenue C. Soula, 31400 Toulouse, France*

Received 31 May 1994; revised 15 June 1995; accepted 6 July 1995

Abstract

A fundamental study of particle detachment of micron-sized glass particles from a model membrane surface is made. The model membrane surface consisted of a cellulose diacetate film which is the polymeric constituent of the hollow fibre membranes used in industrial water treatment. This experimental study aims to analyse the factors leading to the retention of particles on these membranes. We used a hydrodynamic method in which the release of deposited particles was measured under the action of fluid flow. The hydrodynamic force is calculated under well defined hydrodynamic conditions and related to the total adhesive force acting on the particle. We studied the influence of several factors such as, pH, solution salinity, and the effects of adsorbed polymer or non-ionic surfactant on the particles. In the absence of organic solutes adsorbed on the particles, the magnitude of the particle–membrane interaction depended on the pH and the salinity of the aqueous medium, as predicted by the DLVO theory. When adsorbed polymer layers are coated on the surface of the particles, the adhesive force between the particles and the surface was found to be significantly greater than that for bare particles. This contrasted to the decrease in adhesion force observed for particle coated with non-ionic surfactant.

Keywords: Particle–membrane adhesion; Particle removal; Hydrodynamic force; Adhesive force; Colloid fouling

1. Introduction

The study of particle deposition and detachment is of great interest in all filtration processes. It can improve our knowledge of phenomena governing the accumulation of deposits and fouling matter at surfaces or within filter media. Both the hydrodynamic force, usually dominant in the far-field region, and electrochemical forces, dominant in the near field region, are critically important for an understanding of the mechanisms of particle deposition. Here, we focus our attention on the mechanisms leading to the clogging of membranes during a crossflow filtration process. The objective of crossflow filtration is to avoid the build-up of solid particles on the surface of the filter which occurs in classical frontal filtration. The suspension flow is tangential to the filter surface and the wall shear stress effect is assumed to be sufficient to avoid particle accumulation. In fact, aggregates are observed at the surface of the membranes, and it is generally assumed that particle deposition is the main factor responsible for the decreasing filtrate flux and subsequently for membrane fouling.

At a macroscopic level, theoretical hydrodynamic approaches have been carried out by Cox and Brenner [1], Belford and Nagata [2]. They studied the influ-

* Corresponding author.

SSDI 0376-7388(95)00181-6

ence of the inertial and the suction effects on a buoyant spherical particle in a porous tube. Following this, studies were conducted to analyse the physico-chemical forces and the changes in the flow at the microscopic pore size level. Tousi et al. [3] and Durlofski [4] developed models which simulated the deposition of particles up to monolayer coverage. Schmitz [5] developed a statistical model able to simulate multilayer deposition on a porous wall. Experimental studies allow characterization of the fouling tendancies of ultrafiltration and microfiltration membranes. Wandelt [6] visualized and analysed the deposition of model suspensions (chalky bentonite suspension and polystyrene latex particles) on the surface of ultrafiltration membranes. The use of direct and non-destructive nuclear magnetic resonance (NMR) permitted observation of the evolution of deposit formation and compressibility. Gesan [7], Gekas [8], and Persson et al. [9], performed experiments with protein solutions or solutions containing other fouling matter, and detected the fouling effects from the degree of flux recovery. Rautenbach et al. [10] and Blake [11] conducted experiments with model suspensions and used a hydrodynamic force balance to characterize the criteria of deposition of the particles on a membrane surface.

At a microscopic level, investigations were performed by Spielman et al. [12] describing the influence of physico-chemical and hydrodynamic forces on the behaviour of suspended particles close to a wall.

Many authors have considered shear flow without suction. Sharma [13] and Chamoun [14] conducted flow cell and centrifuge experiments to measure a critical hydrodynamic velocity which was defined as the velocity at which 10% of the particles were removed from a flat glass substrate. The critical velocity was found to be influenced by particle size and type, pH and ionic strength. Pelton [15] deposited 5 μm polystyrene spheres inside a glass capillary which was covered with a layer of adsorbed polyethyleneimine (PEI). The effects of pH, molecular weights and concentration of polymer on the sphere–PEI–glass adhesive force were investigated. The adhesion was related directly to bond strength which was lowest at pH = 3 and was greatest at pH = 10. Varennes and Van de Ven [16] reported results using a stagnation point flow technique in a confined impinging jet. They studied the kinetics of deposition and detachment of spherical particles onto and from a glass surface in the presence of cationic polyelectrolyte. The coating of cationic polymer changed the surface charge from negative to positive, which increased the attraction between the surfaces. Original work was carried out by Baudin [17], developing a model particle–membrane surface system. The system consisted of spherical glass particles with the polymeric constituent of ultrafiltration membranes used as the membrane substrate. She conducted flow cell experiments both in the presence and in the absence of macrosolutes on particle and substrate surfaces. The effect of steric repulsion between surfaces coated with the solutes was established.

In this paper, we are particularly interested in the factors leading to the fouling of organic membranes used for drinking water production. Mineral particle deposition on the membrane surface and adsorption of organic solutes within the membrane are believed to be the main factors responsible for decreased flux with time. A model particle–organic solutes–membrane surface system was chosen using glass particles as mineral particles, neutral polymer and non ionic surfactant as organic solutes and a film of cellulose diacetate as the membrane surface. We carry out experiments in order to quantify the net adhesive forces acting on particles bonded on a plane surface under the action of a shear flow. The preliminary results obtained by Baudin can be improved, particularly with respect to the hydrodynamic conditions and the characterisation of the surfaces. Indeed, non-reproducible results are expected from hydrodynamic fluctuations near the wall, and from the presence of roughness on the surface of the particles. Here, results are presented from flow experiments in a specially designed flow cell where hydrodynamic conditions were carefully defined. Special attention was given to the preparation of particle and substrate surfaces to achieve quantitative results.

2. Principle of the hydrodynamic method

A rectangular glass cell with well-defined hydrodynamics was designed. A shear flow was established near the surface wall where particles were deposited. The spherical particles of radius r_p in contact with the plane wall were subjected to a hydrodynamic force F_H calculated by O'neill [18]:

$$F_H = 1.7009 \times 6\pi\mu r_p v(r_p) \quad (1)$$

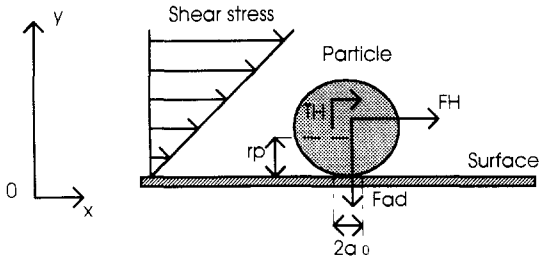

Fig. 1. Torque balance.

where μ is the dynamic viscosity of the fluid, r_p the radius of the particle, and $v(r_p)$ the fluid velocity at a distance r_p from the surface.

The net adhesive force F_{ad} between the particle and the surface, taken normal to the wall, can be found from the summation of the DLVO interaction forces, the inertial lift force and the particle buoyancy. In a situation where polymeric chains are adsorbed on surfaces, we have an additional force which is generally observed to increase the adhesion between the surfaces (Pelton [15], Varennes et al. [19]). The difficulty in calculating the surface forces led to consideration of the global adhesive force F_{ad}. During experiments, particles were observed rolling on the surface. From these observations, it was concluded that the mode of incipient motion responsible for particle release was rolling. For such a release mechanism a torque balance can be used to relate F_{ad} to the tangential hydrodynamic force F_H (Fig. 1). The hydrodynamic torque T_H acting upon a spherical particle exposed to a single shear flow has been calculated by Hubbe [20]:

$$T_H = 1.38 \times F_H \times r_p \tag{2}$$

The torque balance which relates F_H to F_{ad}, is given as:

$$1.38 \times F_H \times r_p = F_{ad} \times a_0 \tag{3}$$

where $2a_0$ is the area of contact between the particle and the collector surface. The measurement of F_H and the estimation of the area of contact $2a_0$ allowed calculation of the net adhesive force F_{ad}.

3. Hydrodynamic conditions

Characterization of the hydrodynamic conditions inside the cell was essential to validate the use of the theoretical expression of the hydrodynamic force F_H [Eq. (1)]. We assume that the fluid is incompressible, has a constant density ρ and viscosity μ, and that the Reynolds number is sufficiently small to use the simplified Stokes' equations. The equations governing the fluid motion are:

$$\nabla P = -\mu \nabla^2 V$$
$$\div V = 0 \tag{4}$$

where, P is the hydrodynamic fluid pressure, and V the fluid flow velocity. The resolution of Stokes' equations of the fluid bounded between two walls separated by a distance $d = 2h$ gives:

$$V = -\nabla P \times \frac{h^3}{3\mu} \tag{5}$$

where h is the half depth separating the two walls.

We assume that the main direction of the flow is tangential to the surface, in the x direction, and we consider the problem as uni-directional. Eq. (5) becomes:

$$\frac{dP}{dx} = -\frac{3\mu}{2h^3} Q \tag{6}$$

and gives a linear relation between the pressure gradient dP/dx, and the flow rate Q. In order to verify the validity of Eq. (6), we performed preliminary measurements of dP/dx with varying the flow rate Q. Two pressure gauges were located near the entrance and the outlet of the cell. The pressure gradient dP/dx was calculated as follows:

$$\frac{dP}{dx} = \frac{P_i - P_o}{x_i - x_o},$$

where P_i is the inlet pressure, P_o the outlet pressure, and $(x_i - x_o)$ the distance between the two pressure gauges. The results are reported in Fig. 2, and showed a linear relation between the pressure gradient and the flow rate. Next, the half depth of the channel h was calculated under Eq. (6) with the measured values of dP/dx and Q. The calculated value ($h = 1$ mm ± 0.1) agreed well with the known value ($h = 1$ mm for our rectangular cell). We can assume to a good approximation that Poiseuille flow is established inside the experimental cell. We ensure that the fluid flow is fully developed in the channel at a distance greater than the length L_e. The calculation of the establishment length

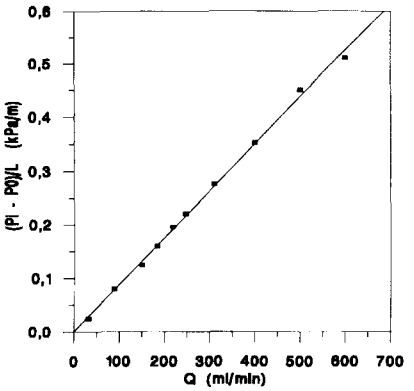

Fig. 2. Linear law between the pressure gradient dp/dx and the flow rate Q.

flow was done using the Karman–Polhaussen integral method applied to a rectangular cell:

$$L_e = 0.09 \times Re \times h \tag{7}$$

where Re is the Reynolds number of the flow:

$$Re = \frac{U_m \times 2h}{\nu} \tag{8}$$

υ is the kinematic viscosity of the fluid, and h the half depth of the cell channel. U_m is the mean velocity of the flow defined as: $U_m = Q/S$, where Q is the flow rate and S the cross sectional area of the cell. At distances greater than L_e, the velocity profile of the fluid is parabolic with respect to channel depth, and the velocity at a distance $y = r_p$ is given by:

$$\upsilon(r_p) = 1.5 \times \left[1 - (1 - \frac{r_p}{h})^2\right] \times U_m \tag{9}$$

Moreover, we assumed that the particles were small enough to be held inside the laminar sublayer in which the velocity gradient of the fluid is almost linear. Indeed, the ratio $r_p/h = 0.02 < 1$ ($r_p = 20$ μm, h = 1 mm), and Eq. (4) can be written as:

$$\upsilon(r_p) = \frac{3r_p}{h} \times U_m \tag{10}$$

The hydrodynamic force acting on particles is calculated using Eqs. (1) and (10), for the different values of the flow rate Q. The flow regimes considered are kept laminar ($Re < 500$) and the hydrodynamic force calculated was in the range of 10^{-11}–10^{-8} Newtons.

3.1. The inertial lift force

The expression which predicts the inertial lift force $F_\perp$ on a sphere in a linear shear stress field near a flat infinite has been calculated by Cherukat [21]:

$$F_\perp = 9.22 \times r_p^2 \times \upsilon(r_p)^2 \tag{11}$$

The ratio between the lift force $F_\perp$ and the drag force F_H provides a measure of the relative significance of inertial and viscous effects:

$$\frac{F_\perp}{F_H} = \frac{9.22 \times r_p^2 \times \upsilon(r_p)^2}{1.7009 \times 6\pi\mu r_p \upsilon(r_p)} = 0.14 \times Re_p \tag{12}$$

where

$$Re_p = \frac{r_p \times V(r_p)}{\nu}$$

is the local Reynolds number based on particle radius. The local Reynolds number is in the range of 10^{-2}–1, and since $F_\perp < F_H$, the lift force can be neglected.

4. Experimental

4.1. Experimental set-up

The experimental apparatus consists of a fluid reservoir, a peristaltic pump, a pulse damper, two pressure gauges, a flow cell, a combination of a microscope-camera-video image processing system for the visualization and the counting of the particles, a particle injection syringe, a water collection syringe, a flow meter. The fluid flowing through the cell was distilled water. A schematic diagram of the experimental set-up is shown in Fig. 3.

4.2. Materials

Flow cell

The rectangular cell was composed of two glass plates held together with aluminium clamps. The two glass plates were separated by means of a hollowed out Plexiglas plate for channeling the fluid flow. The experimental glass cell was 2 mm in depth, 30 mm in width, and 120 mm in length.

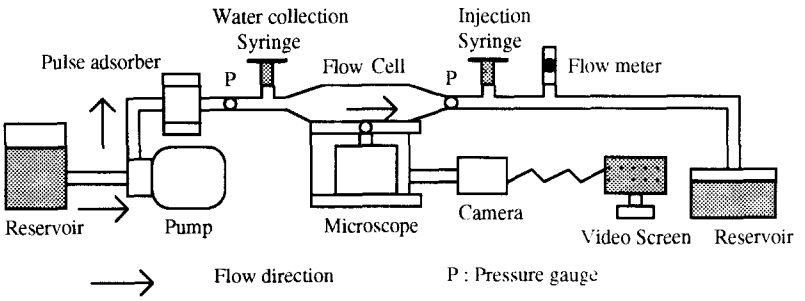

Fig. 3. Experimental set-up.

Particles

The glass particles were purchased from Verre et Industrie company. They had a radius of 20 μm. There was a 10% standard deviation in particle size. Their specific density was 2.5×10^3 Kg/m^3. The chemical composition was given as: S_iO_2: 66%, Na_2O: 15%, Ca0: 7%, Al_2O_3: 5%, B_2O_3: 3%, ZnO: 2%, Mg0: 1%, K_2O: 1%.

The dissociation of silanol groups (SiOH) on the particle surface are responsible for their negative charge according to:

$$SiOH \rightleftarrows SiO^- + H^+$$

The zeta potentials of the glass particles were determined from the mobility measurements using a Malvern Zetasizer 4 microelectrophoresis apparatus. The general equation between the particle mobility and the zeta potential is given by Smoluchowski's equation:

$$u_E = \frac{\zeta_p \times \varepsilon}{\mu} \qquad (13)$$

where u_E is the electrophoretic mobility, ζ_p the zeta potential of the particles, ε the dielectric constant of the suspending fluid, and μ the fluid viscosity. The values of zeta potentials are reported in Table 1, at different pH values and salinities, adding acid (HCl), base (NaOH), or salt (NaCl), in the solution. The results were in agreement with those in the literature [22].

Table 1
Zeta potentials of glass particles at various pH and salintiy

	pH = 5	pH = 7	pH = 9
NaCl = 10^{-3} M	$\zeta_p = -30$ mV	$\zeta_p = -40$ mV	$\zeta_p = -42$ mV
NaCl = 10^{-1} M	$\zeta_p = -20$ mV	$\zeta_p = -24$ mV	$\zeta_p = -28$ mV

Model membrane

Cellulose diacetate (CDA) was chosen as the model surface since it is one of the major components in manufactured hollow fibre membranes. A thin layer of CDA covered the bottom of the glass cell and constituted the model membrane surface. The CDA surface was negatively charged in the range of pH 5–9, and the value of the CDA zeta potential was taken as ~ -5 mV (Baudin [17]).

Organic solutes

The neutral polymer adsorbed on the particles was polyethylene oxide (PEO) with mean molecular weights of 35×10^3, 200×10^3 and 600×10^3. The non-ionic surfactant used in our experimental study was triton X-100. The surfactant was coated on the particles at the critical micellar concentration $C = 2.9\times10^{-4}$ mol l^{-1}.

The glass particles and the organic solutes were used to model respectively the mineral particles and the organic matter contained in the deposits encountered on the surface of the hollow fibre membranes.

4.3. Experimental procedures

Cleaning procedure

Rigorous cleaning of particles was necessary to obtain reproducible results. The presence of asperities on particle surfaces can prevent their release from the surface. The glass particles were cleaned by treating them with a concentrated nitric acid solution (0.1 mol l^{-1}) for 12 h and subsequently rinsing them with large quantities of distilled water. This treatment allowed reproducible results to be obtained, with a deviation of 10% in the measured hydrodynamic force. Scanning electron microscopy photographs was carried out on the treated particles. The results showed no cracks or

features. It was concluded that the scale of roughnesses was below 10 nm.

Adsorption of the organic solutes

A stock solution was prepared by adding the polymer or the surfactant to distilled water. The stock solution was stirred for 12 h. The concentrations of POE contained in the stock solution varied from $C = 50$ mg l^{-1} to 1000 mg l^{-1}. The surfactant was adsorbed on the surface of the particles at $C = 2.9 \times 10^{-4}$ mol l^{-1}. The glass particles were then suspended in a reservoir which contained the polymer or surfactant stock solution. A small fraction of the suspension was taken from the stock solution to give a final solution concentration of $C = 0.1$ g l^{-1}.

Experiment

Initially distilled water circulated through the experimental system and filled the glass cell. This was replaced with the electrolyte solution. A syringe placed downstream of the cell was then used to inject particles into the cell. A second syringe, placed upstream of the flow cell, collected the displaced liquid. The region of interest was observed through an optical microscope, and recorded using a video system. The particles were allowed to settle for one hour. The initial number of particles N_0 was then counted at a very low solution flow rate. The flow rate Q was increased incrementally, and 10 min after it has been adjusted, the number of particles remaining N_p was determined.

5. Results and discussion

The results obtained are plotted as the fraction of particles attached to the surface N_p/N_0, versus the applied hydrodynamic force F_H. The initial number of deposited particles N_o varied from 150 to 200. The mean values of F_H (for 10 experiments) are reported on the curves. The error (ΔF_H) in F_H measurements is $\sim 10\%$.

5.1. Experimental observations

We observed in our experimental study that a $\sim 10\%$ of the particles remained on the collector surface. Moreover, particles were not all simultaneously removed from the surface, but rather the number of particles released increased with increasing hydrodynamic force.

5.2. Influence of pH and ionic strength

Fig. 4 and Fig. 5 show results from experiments performed in the absence of organic solutes, at various pH values and salinities. It can be seen that from these curves that decreasing pH (acid pH) or increasing ionic strength, resulted in a higher hydrodynamic force needed to release particles from the surface.

These results are in agreement with DLVO theory which describes the energy of interaction between two charged surfaces in a polar medium. According to the classical DLVO theory the net energy of interaction V_T

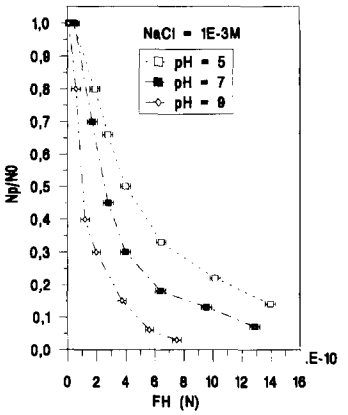

Fig. 4. Hydrodynamic force versus the rate N_p/N_0 of particles deposited on the CDA surface. Influence of the pH of the solution. NaCl = 10^{-3} mol l^{-1}; $r_p = 20$ μm; $N_0 = 200$.

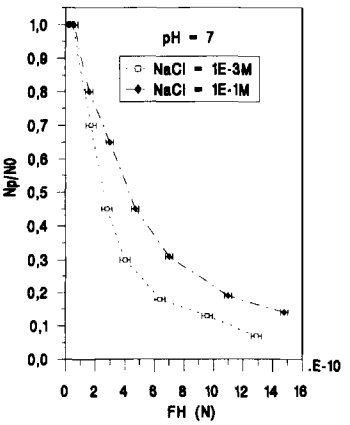

Fig. 5. Influence of the ionic strength of the solution on the rate of particles N_p/N_0 resting on the CDA surface. pH = 7; $r_p = 20$ μm; $N_0 = 200$.

is the summation of two contributions, the attractive Van der Waals energy, and the repulsive electric double layer energy:

$$V_T = V_{vdw} + V_{el} \quad (14)$$

For a sphere, radius r_p, separated by a distance h_0 from a flat plate, the expression of the Van der Waals potential is given by:

$$V_{vdw} = -\frac{A_{123} r_p}{6h_0} \quad (15)$$

where A_{123} is the Hamaker constant of the glass–water–cellulose diacetate system.

The electric double layer energy is calculated by the following equation (Hogg et al. [22]):

$$V_{el} = \frac{\varepsilon \varepsilon_0 r_p (\zeta_p^2 + \zeta_s^2)}{4k_B T} \times \left[\frac{2\zeta_p \zeta_s}{\zeta_p^2 + \zeta_s^2} \times \ln\frac{1+\exp(-kh_0)}{1-\exp(-kh_0)} + \ln(1-\exp(-2kh_0))\right] \quad (16)$$

where ε is the dielectric constant of the fluid, ε_0 the permitivity of vacuum, k_B the Boltzmann constant, T the absolute temperature, ζ_p and ζ_s the zeta potentials, respectively, of the particles and surface, and κ the inverse Debye length.

For aqueous solutions of symmetric electrolyte (1:1), at $T = 25°C$, κ is given by:

$$\kappa = 0.328 \times 10^{10} \times \sqrt{I} \quad (17)$$

where I is the ionic strength of the solution. The Debye reciprocal length κ^{-1} is an important parameter for quantitative description of the double layer, and is often regarded as the thicknesss of the double layer.

The effects of the pH are directly based on the increase or decrease of the zeta potential of particles and CDA surfaces. Both glass particles and the CDA surface are negatively charged in the range of pH [5–9]. The absolute values of zeta potential are lower at acid pH and at high ionic strength (Table 1). At acid pH, the electric double layer repulsion [16] is weaker, resulting in stronger adhesion of particles to the surface. The same tendency is observed with increasing the salt concentration. Increasing the salt concentration decreases the double layer thickness, i.e. κ^{-1}, and hence the zeta potential which results in less repulsion between the interacting surfaces. We show in Fig. 6

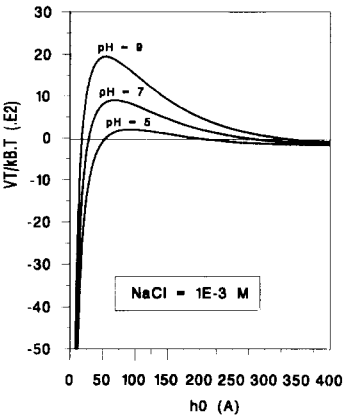

Fig. 6. The interaction energy V_T/k_BT versus the distance h_0 separating the particle and the surface. Influence of the pH of the solution. NaCl = 10^{-3} mol l^{-1}; $r_p = 20$ μm.

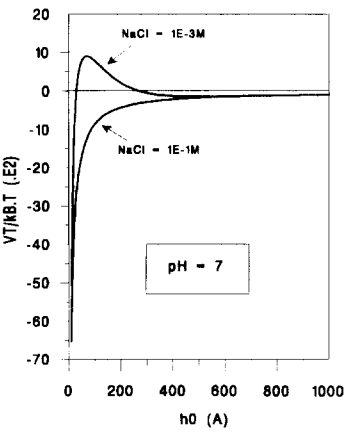

Fig. 7. Influence of the ionic strength of the solution on the dimensionless interaction energy V_T/k_BT pH = 7; $r = 20$ μm.

and Fig. 7, the variation of the dimensionless interaction energy V_T/k_BT, as a function of separation distance h_0 for different pH values and salinities. The presence of a maximum, i.e. an energy barrier, determines the conditions for particle deposition. It can be seen that the decreasing the pH (Fig. 6) or increasing the salinity (Fig. 7) reduces the height of the interaction energy barrier V_T.

5.3. *Influence of neutral polymer adsorption*

The polyethylene oxide adsorbed on the particles has mean molecular weights M_p of $35 \times 10_3$, $200 \times 10_3$ and $600 \times 10_3$. The POE concentrations vary from $C = 0$ to 10^3 mg l^{-1}. Fig. 8 shows the hydrodynamic force necessary to release 50% of particles from the surface, i.e.

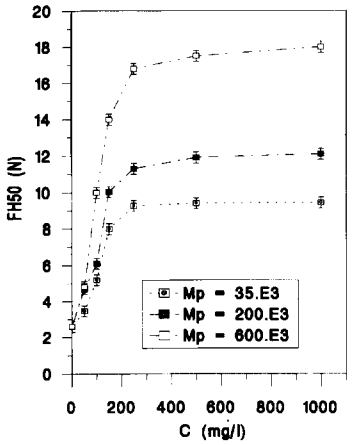

Fig. 8. The hydrodynamic force F_{H50} as a function of the polymer concentration C, at different molecular weights: $M_p = 35 \times 10^3$, 200×10^3 and 600×10^3. pH = 7; NaCl = 10^{-3} mol l^{-1}; $r_p = 20$ μm; $N_0 = 180$.

F_{H50}, as a function of polymer concentration C and molecular weight M_p, at pH 7 and at an ionic strength of 10^{-3} mol l^{-1}. At each molecular weight, the hydrodynamic force F_{H50} showed a strong dependence on POE concentration, increasing rapidly with increasing POE concentration up to $C \sim 250$ mg l^{-1}. For POE concentrations > 250 mg l_{-1}, F_{H50} reached a maximum value and became independent of further increases in POE concentration. The maximum F_{H50} increased with increasing M_p. Increasing the concentration and the mean molecular weight (which extends the length of the polymeric chains) of the adsorbed polymer increases the number of bridges between the surfaces. Hence, it strengthens the adhesive force between particle and CDA surface. At the three different molecular weights, the maximal hydrodynamic force F_{H50} was obtained at ~ 250 mg l^{-1}. This concentration corresponds to saturation of the particle surface by the polymeric chains during the adsorption procedure. For POE concentrations > 250 mg l^{-1}, the excess polymer stays in solution and is not adsorbed on particle surface.

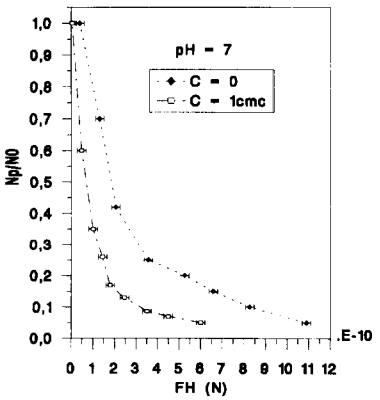

Fig. 9. Influence of the presence of triton adsorbed at $C = 1$ cmc on particle surface. Comparison with the situation where $C = 0$ (without surfactant). pH = 7; $r_p = 20$ μm.; $N_0 = 150$.

The polymeric chains are adsorbed on the silica particles by hydrogen bond formation between the silanol groups (SiOH) on the glass particles and the ether group of the polyethylene oxide. When particles are deposited on the CDA surface the polymeric chains adsorbed on particles form molecular bridges with the surface. The high affinity of the polymer for the particle and CDA surfaces leads to a strong intermolecular adhesion between the surfaces.

5.4. *Influence of surfactant adsorption*

Finally, we consider the effects of a non ionic surfactant, the triton X-100, on the adhesive interaction between particles and model membrane surface. We studied the release of particles as a function of applied F_H for both bare and surfactant covered particles. The results are presented in Fig. 9. It shows that surfactant covered particles are removed from the surface more easily than bare particles, evidenced by the lower values of hydrodynamic force. The reduction in adhesion energy due to the presence of triton can be explained by a number of factors. The hydrophobic tails of the triton are adsorbed on particle surface and the membrane surface is exposed to the hydrophilic head group of the surfactant. The presence of triton induces steric effects between surfaces and a substantial decrease in adhesion between particles and membrane surface is observed. We assume also, that there is a reduction in the attractive Van der Waals force due to surfactant adsorption which should be taken into account. The presence of surfactant tails increases the separation distance h_0 between the surfaces, and consequently decreases the Van der Waals interaction energy.

6. Estimation of the adhesive force fad

Measured values of F_{H50}, the hydrodynamic force necessary to release 50% of particles, were compared

Table 2
Comparison of F_{H50} and F_{ad}. Experimental conditions: absence of solutes adsorbed on particles; various pH and salinity; $a_0 = 4 \times 10$ m; $r_p = 20$ μm

Absence of organic solutes				
Experimental Conditions	pH = 5 NaCl = 10^{-3} M	pH = 7 NaCl = 10^{-3} M	pH = 9 NaCl = 10^{-3} M	pH = 7 NaCl = 10^{-1}
F_{H50} (N)	3.4×10^{-10}	2.1×10^{-10}	1.05×10^{-10}	3.3×10^{-10}
F_{ad} (N)	2.34×10^{-7}	1.45×10^{-7}	0.62×10^{-7}	2.28×10^{-7}

Table 3
Values of F_{H50} and F_{ad} at various experimental conditions. POE adsorbed at $C = 250$ mg l^{-1}, at various molecular weights. Triton adsorbed at the cmc $a_0 = 4 \times 10^{-8}$ m; $r_p = 20$ μm

POE adsorbed on particles				Triton adsorbed at $C = 1$ cmc
Molecular weight	$M_p = 35 \times 10^3$	$M_p = 200 \times 10^3$	$M_p = 600 \times 10^3$	
F_{H50} (N)	5.6×10^{-10}	11.16×10^{-10}	17.1×10^{-10}	0.9×10^{-10}
F_{ad} (N)	3.9×10^{-7}	7.7×10^{-7}	11.8×10^{-7}	0.62×10^{-7}

to values of F_{ad}, calculated from Eq. (3), for the range of experimental conditions. The results are shown in Table 2 for bare particles, and in Table 3 for particles adsorbed with solutes. The contact radius for 20 μm glass particles calculated was taken as $a_0 \sim 4 \times 10^{-8}$ m. The value of a_0 was taken from Sharma et al. [13]. They calculated the contact radius of glass particles deposited on a planar surface, for different particle diameters. The basis of the calculation was Hertz theory [23], which describes the deformation of the particle under surface forces acting in and around the contact region. The authors assumed that the Hertz's solution was valid, even for hard surfaces as glass surfaces.

It can be seen that the calculated values of F_{ad} are significantly larger than F_{H50}. The ratio of F_{ad} to F_{150} ~ 700. The surface forces are assumed to be responsible for the attachment of particles to the collector surface and their effect is strongest in the area of contact between the particles and the surface. However, calculation of F_{ad} is dependent on the estimation of a_0. The presence of surface roughnesses can be expected to play an important role, changing significantly the value of a_0. Surface defects on a scale up to ~ 10 nm were revealed on the particles. It could explain that $\sim 10\%$ of particles are remained on the surface, and that particles are removed gradually. Consequently, surface roughnesses on both particles and the CDA film could be important in determining the nature of particle release.

7. Conclusions

The global adhesive force between colloidal particles and a planar surface has been determined from the experimentally measured hydrodynamic force, which is incorporated in a torque balance. The adhesive force was greater than the hydrodynamic force by nearly three orders of magnitude. The experiments using the hydrodynamic technique allow a quantification of both, the effect of the surfaces charge and the influence of polymers or surfactants, on the particle–CDA surface interaction. Decreasing the pH or increasing the ionic strength increased the adhesive force between particles and the CDA surface. When particles were coated with POE, it was shown that the presence of polymeric chains adsorbed on the surfaces increased the adhesive interaction. This could explain difficulties in removal of the fouling cake which accumulates on a membrane surface during a real filtration operation. Finally, the interest in using non-ionic surfactant (triton X-100) coated on particles is pointed out. The presence of surfactant on particle surfaces caused a weaker adhesion force and consequently greater removal of particles

from the surface. This could be useful for reducing membrane fouling.

8. List of symbols

A_{123}	Hamaker constant (J)
a_0	radius of contact between sphere and collector surface (m)
C	concentration of organic solutes (mg/l)
F_{ad}	total adhesive force (N)
F_H	hydrodynamic force (N)
$F_\perp$	inertial lift force (N)
h	half cell depth (m)
h_0	distance of separation between the sphere and the surface (m)
I	ionic strength of the solution (mol l^{-1})
k_B	Boltzmann constant (J/K)
L_e	establishment length (m)
M_p	molecular weight of the polymer
P	hydrodynamic fluid pressure vector (Pa)
P_i	pressure at cell inlet (Pa)
P_o	pressure at cell outlet (Pa)
Q	flow rate (m^3/s)
Re	Reynolds number
Re_p	local Reynolds number
r_p	radius of the particle (m)
S	cross sectional area of cell (m^2)
T	absolute temperature (K)
T_H	hydrodynamic torque (N/m)
U_m	mean velocity of the flow (m/s)
u_E	electrophoretic mobility of particles ($m^2\ s^{-1}\ V^{-1}$)
V	fluid flow velocity vector (m/s)
V_c	critical velocity
V_{el}	electric double layer potential (J)
V_T	net energy of interaction (J)
V_{vdw}	Van der Waals potential (J)
$v(r_p)$	fluid velocity at a distance $y = r_p$ from the surface (m/s)
$x_i - x_0$	distance between the two pressure gauges (m)
ε	dielectric constant of the fluid
ε_0	permitivity of vacuum (C^2/J m)
κ	Debye length (m^{-1})
μ	dynamic viscosity of the fluid (kg/m/s)
ζ_p	zeta potential of the particle (mV)
ζ_s	zeta potential of the surface (mV)

References

[1] R.G. Cox and H. Brenner, The lateral migration of solid particles in Poiseuille flow, Chem. Eng. Sci., 23 (1968) 147–173.

[2] G. Belford and N. Nagata, Fluid mechanics and crossflow filtration: some thoughts, Desalination, 53 (1985) 57–59.

[3] S. Tousi, F. Henri and T. Ariman, Numerical investigation of particle collection in fibrous filters, in T. Ariman and T.N. Veziroglu (Eds), Proc. Int. Symp. Workshop in Particulate and Multiphase Processes, Fine Particle Society, Miami, FL, 1985, pp. 1–3.

[4] L.J. Durlofski and J.F. Brady, Dynamic simulation of bounded suspensions of hydrodynamically interacting particles, J. Fluid Mech., 200 (1989) 39–67.

[5] P. Schmitz, D. Houi and B. Wandelt, particle aggregation at the membrane surface in crossflow microfiltration, J. Membrane Sci., 84 (1993) 171–183.

[6] B. Wandelt, D. Houi and P. Schmitz, Micro and ultrafiltration of dilute suspensions: NMR microimaging of deposit formation in hollow fibers, in P. Aimar and P. Aptel (Eds.), Proc. Euromembrane, Recents Progres en Genie des Procedes, 6 (1992) 251–256.

[7] G. Gesan, U. Merin, G. Daufin and J. Maugas, Performance of industrial microfiltration plant for defatted rennets whey, in A. Burggraaf, J. Charpin and L. Cot (Eds.), Inorganic Membranes, Proceedings of ICIM2-91-trans Tech Publications Zurich, 1991, pp. 307–312.

[8] V. Gekas and B. Hallström, Microfiltration membranes, crossflow transport mechanisms and fouling studies, Desalination, 77 (19890) 195–218.

[9] K.M. Person, P. Dejmek and G. Trägårdh, Fouling behaviour on four different microfiltration membranes, J. Membrane Sci., 76 (1993) 61–71.

[10] R. Rautenbach and G. Schock, Ultrafiltration of macromolecular species and crossflow microfiltration of colloidal suspensions. A contribution to permeate flux calculations, J. Membrane Sci., 36 (1988) 231–342.

[11] M.J. Blake, I.W. Cumming and N. Streat, Production of steady state crossflow filtration using a force balance model, J. Membrane Sci., 68 (1992) 205–216.

[12] L.A. Spielman and S.L. Goren, Capture of small particles by London forces from low speed liquid flows, Env. Sci. Technol., 4 (1970) 135–140.

[13] M.M. Sharma, Factors controlling the hydrodynamic detachment of particles from surfaces, J. Colloid Interface Sci., 149(1) (1992) 121.

[14] H. Chamoun, R.S. Schechter and M.M. Sharma, Hydrodynamic forces necessary to release non-Brownian particles attached to a surface, 195th National Meeting of the American Chemical Society, Toronto-Ontario, Canada, June 1988.

[15] R.H. Pelton, Factors influencing the adhesion of polystyrene spheres attached to Pyrex by polyethyleneimine in aqueous solution, J. Colloid Interface Sci., 99(2) (1984) 387.

[16] S. Varennes and T.G.M. Van de Ven, Physico chemicals hydrodynamics, deposition and detachment of latex particles at glass surfaces exposed to flow, J. Colloid Interface Sci., 9(3/4) (1987) 537–559.
[17] I.Baudin, Thesis, University Pierre and Marie Curie, Paris VI, France, 1991.
[18] M.E. O'Neill, A sphere in contact with a plane wall in a slow linear shear flow, Chem. Eng. Sci., 23 (1968) 1293.
[19] S. Varennes and T.G.M. Van de Ven, Effects of polyelectrolyte on the deposition and detachment of colloidal particles subjected to flow, Colloids Surfaces, 33 (1988) 63.
[20] M.A. Hubbe, Theory of detachment of colloidal particles from flat surfaces exposed flow, Colloid Surfaces, 12 (1984) 151–178.
[21] P. Cherukat and J.B. McLaughlin, The inertial lift on a rigid sphere in a linear shear flow field near a flat wall, J. Fluid Mech., 23 (1994) 1–18.
[22] H. Chamoun, A Theoretical and Experimental Study of the Release of Non-Brownian Particles from Surfaces, Thesis, University of Texas, Austin, 1989.
[23] H. Hertz, Theory of Elasticity, S.P. Timoshenko and J.N. Goodier Editions, McGraw-Hill, New York, 1970.